The Abdus Salam
International Centre for Theoretical Physics

United Nations
Educational, Scientific and
Cultural Organization

IAEA
International Atomic Energy Agency

2167-31

Advanced School on Direct and Inverse Problems of Seismology

27 September - 8 October, 2010

Precisely relocated hypocentres, focal mechanisms and active orogeny in Central Taiwan

Francis T. Wu
State University of New York
Binghamton
New Yor
USA

Precisely relocated hypocentres, focal mechanisms and active orogeny in Central Taiwan

F. T. WU[1], C. S. CHANG[2] AND Y. M. WU[2]
[1]*Department of Geological Sciences, State University of New York, Binghamton, NY 13902 USA (e-mail: wu@binghamton.edu)*
[2]*Central Weather Bureau, Taipei, Taiwan*

Abstract: The 1999 Chi-Chi earthquake series occurred in Central Taiwan, where ongoing mountain building is most active. The pre- and post-Chi-Chi seismicity helps to clarify the internal orogenic activity. The 27 000 earthquakes from the 1993–2002 catalogues have been relocated with greater precision. By associating the seismicity with focal mechanisms, many structures inside the orogen have been mapped. Among them are a steeply dipping thrust fault in the deep crust; a 50-km-long left-lateral strike-slip fault in the south; and an Eastern Central Range NNE-striking normal fault. While the deep crustal thrust appears to contribute to the root-building, the southern strike-slip slip fault accommodates the main-shock fault motion, and the Eastern Central Range normal faulting probably occurs mainly after a major western Taiwan thrust type earthquake. Much of the Backbone Range and the Eastern Central Range were seismically quiescent before and after the Chi-Chi earthquake. The contrast in the seismicity of the Central Range and the surrounding regions implies different material behaviour in these different regimes of the orogen.

Taiwan is an active orogen created from the convergence between the Eurasian and the Philippine Sea plate (Fig. 1). The rate of convergence is 70 mm/year, based on NUVEL-1 of De Mets *et al.* (1990), and recent estimates from GPS measurement are about 8 cm/year (Yu *et al.* 1999). This convergence is nearly totally absorbed in the shortening across the Taiwan, as the rate decreases from over 50 mm/year on the east coast to essentially zero in the Coastal Plain. The total rate of uplift is estimated to be in excess of 5 mm/year in the last million years, with a 1 cm/year rock uplift rate in the last 30 years (Liu, C. C., pers. comm., 2002). The seismicity in the orogen is coupled with these high rates of crustal movement. Since seismicity is a response to the tectonic stresses, the location and the focal mechanisms of earthquakes will provide information concerning the stresses, as well as giving the kinematics of faults. In this paper we utilize a relatively new and effective method to relocate more precisely the hypocentres of earthquakes (Waldhauser and Ellsworth 2000). The better-resolved hypocentre distribution forms the basis from which zones of active deformation can be mapped. Certainly, the presence of seismicity is an unmistakable sign of brittle deformation, but clearly defined zones of seismically quiescence in the orogen, especially in between regions of high activity, call for understanding of possible rheological behaviour of rocks – brittle or ductile – in the orogen, and the thermal conditions there. In these studies, the precision of the hypocentral location is the key; only with precise locations can the correlation of the clear patterns of seismicity with known geological entities, such as major faults, crustal roots and so on, be explored.

A detailed seismicity study in Taiwan is made feasible because of a number of factors. Foremost among them is the timely upgrade of the seismic network. The Central Weather Bureau (CWB) seismic network evolved in stages from a historical analogue network in the late 1890s to the present digital network (Yeh *et al.* 2000). For the most recent major overhaul, completed in 1991, the number of stations was doubled, and the network was switched to digital technology (Rau *et al.* 1996). In an area of 36 000 km^2, there are 72 stations, with interstation spacing varying from a few kilometres to about 30 km (Fig. 2). On the average, more than 15 000 events are located every year, but most of them were located offshore of eastern Taiwan. In central Taiwan, where the mountain ranges are relatively high (reaching nearly 4000 m at the highest) and the orogeny is known to be most active the seismicity had been relatively low, historically as well as in the recent years. From 1991 through 19 September 1999, there were few noticeable

From: MALPAS, J., FLETCHER, C. J. N., ALI, J. R. & AITCHISON, J. C. (eds) 2004. *Aspects of the Tectonic Evolution of China*. Geological Society, London, Special Publications, **226**, 333–354.
0305-8719/04/$15

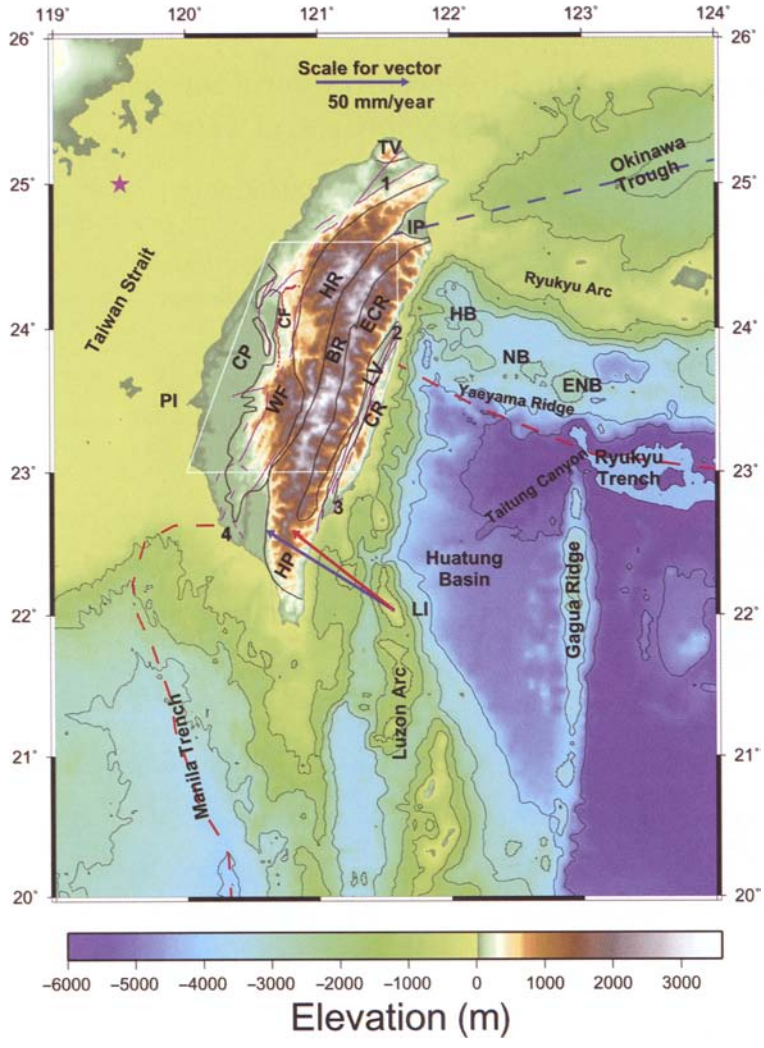

Fig. 1. Plate tectonics in the vicinity of Taiwan. The two-letter codes marking the physiological/geological regions are: CR, Coastal Range; ECR, East Central Range; BR, Backbone Range; HR, Hsueshan Range; WF, Western Foothills; CP, Coastal Plain; HP, Hengchun Peninsula; HB, Hoping Basin; NB, Nanao Basin, and ENB, East Nanao Basin. Place names are: 1, Taipei; 2, Hualian; 3, Taitung; 4, Kaohsiung; PI, Penghu Islands and LI, Lanhsu Island. The boundary between CP and WF is often viewed as the 'deformation front', i.e. the western limit of collision-related deformation, although the Taiwan Strait is actually active, as shown by the occurrence of a large earthquake (marked by a star; *Mc*.8). The arrows centred on the Lanhsu island south-east of Taiwan are the plate motion vector predicted by NUVEL-1 (the red vector) and the motion vector measured by GPS (red vector; Yu *et al.* 1997). The dashed red lines mark the approximate positions of the plate boundaries. The thin red line marks the Chelungpu Fault (CF) and thin magenta lines the other 'active faults'; the fault west of CF is the Changhua Fault. Our area of interest is indicated by the outlined box, extending from the Coastal Plain in the west to the Coastal Range.

events in the study area (between 23°N and 24°N in central Taiwan). Then, on 20 September 1999, the Chi-Chi earthquake ($M_w = 7.6$) occurred; more than 20 $M_w > 6$ (NEIC/USGS) and over 20 000 M > 2 aftershocks followed. The seismic voids in this region were filled, and new seismicity patterns developed. Some of the earthquake zones more clearly distinguishable before the Chi-Chi event in fact disappeared after the main-shock, and the aftershocks occurred not only in the main rupture zone, but even skipped the high Backbone Range and occurred in the

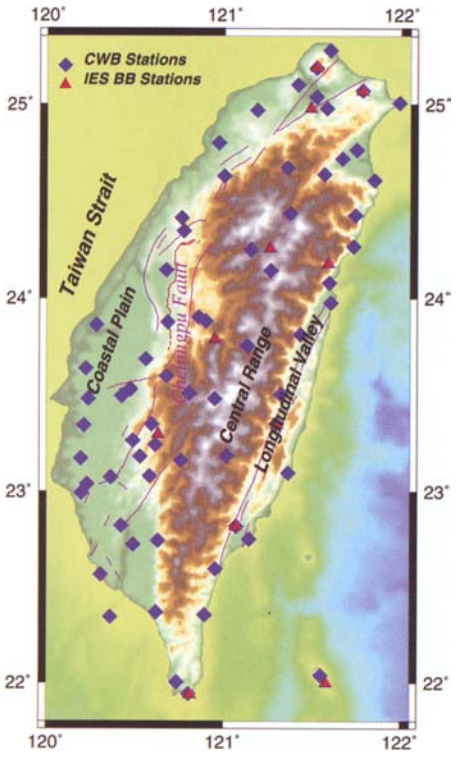

Fig. 2. Locations of the Central Weather Bureau (CWB) and Institute of Earth Sciences (IES), Academia Sinica, seismic stations. The diamonds indicate the CWB narrowband stations, and the squares the IES broadband stations; phase arrival times are from the CWB network, and most of the focal mechanisms used in this paper are from IES stations.

Eastern Central Range, a very low seismic region before the main-shock.

In addition to the short-period CWB network, appropriate for mapping detailed seismicity, the Broadband Array for Taiwan Seismology (BATS) network data are routinely used in the determination of the focal mechanisms of $ML > 3.5$ events. The focal mechanisms derived from waveform inversion are generally more robust than the short-period first-motion solutions (Kao *et al.* 2002). For the large earthquakes ($M > 5.5$), Harvard and USGS focal mechanism solutions are also available. Together with the seismicity, the motions along the fault internal to the orogen can be assessed using these mechanisms.

Seismicity has previously been used in studying the Taiwan orogeny. The most recent work by Carena *et al.* (2002) proposed the presence of a detachment fault by clustering seismic data on to perceived planar structures. Previously, Tsai *et al.* (1977) mapped plate tectonics around Taiwan on the basis of seismicity, and Wu *et al.* (1989; 1997) included seismicity in their overall studies of Taiwan tectonics. They identified zones of seismic quiescence and activity, and associated them with crustal rheology. However, the relocation of hypocentres and the aftershocks of the Chi-Chi earthquake provide better data on known and unknown structures. Although the time window of our good seismicity data is quite short (actually from July 1993 through 2001) a number of significant points regarding the orogenic processes can be addressed.

Tectonics and geology of Taiwan

The plate-tectonic framework and tectonic units are shown in Figure 1. The Philippine Sea plate subducts toward the north along the Ryukyu Trench, and the Eurasian plate subducts toward the east along the Manila Trench. However, the Ryukyu Trench as a bathymetric low disappears west of 123°E, offshore of east Taiwan, and the Manila Trench loses its definition offshore of SW Taiwan north of 21.5°N. As a result, the plate boundaries shown in Figure 1 are only approximate in the immediate vicinity of Taiwan. The section of Taiwan in between the two ends of the boundaries depicted in Figure 1 is the most active section, and the Chi-Chi earthquake occurred in this area. As mentioned earlier, in between the subduction zones the convergence between the Philippine Sea plate and the Eurasian plate appears to be totally absorbed by shortening. The relative motion between Lanhsu, an extinct volcanic island offshore of southeastern Taiwan, and the Penghu Islands in the Taiwan Strait, is about 8 cm/year according to GPS data, slightly larger than the NUVEL-1 prediction (Yu *et al.* 1999; Fig. 1). This situation is in contrast to a typical cross-section across the middle part of the Andes in South America, where shortening takes up only 10–15 mm/year of the total convergence of 70 mm/year between the Nazca and South American plate, while subduction eventually consumes the rest of it (Norabuena *et al.* 1998).

The geology of Taiwan is often represented in a two-dimensional section, and for this paper such a method is adequate. Thus, starting from the east, and moving onshore from the Philippine Sea basin, the Coastal Range is encountered first. It is a telescoped ensemble including all the materials between the former Luzon volcanic arc and the trench (*Terrestrial, Atmospheric and Oceanic Sciences* 1987). Separating the Coastal Range from the Central Range to the west is the Longitudinal Valley (LV), for some time a

depositional trough of continental sediments between two topographical highs. In the part of the Central Range just west of the LV, Mesozoic metamorphic rocks are exposed (ECR in Fig. 1); this is overlain by a suite of Eocene–Miocene sediments to the west; these rocks have been metamorphosed to slates, in what is usually called the Backbone Range (BR in Fig. 1). Further west is the Hsuehshan Range, which is well developed in the north but tapers out toward the south (HR in Fig. 1); the strata are Eocene–Oligocene in age, but are folded and less metamorphosed than the BR rocks. Neogene rocks underlie the Western Foothills. The boundaries between geological units are mostly faults. The major ones are the Longitudinal Valley fault(s), a left-lateral oblique thrust fault zone, and the Lishan fault – the boundary between the Backbone Range and the Hsuehshan Range. Although the Lishan fault is recognized by some (Ho 1988) as a major fault, based on the differences in lithology, age of strata, grades of metamorphism and styles of deformation (Lee *et al.* 1997), it is not shown on the most recent geological map of Taiwan (Central Geological Survey, Taiwan 2000). The Lishan Fault is actually an important boundary for seismicity, as we shall show later. Between the Foothills and the Coastal Plain is the Chelungpu Fault, and further west is the Changhua Fault (Fig. 1). Incidentally, the Changhua Fault is often depicted as the 'deformation front', in other words, the western limit of the orogenic deformation. But the Taiwan Strait is also seismically active, even though the tectonics may be dominated by N–S tension (Kao and Wu 1996).

The subsurface structures of Taiwan are complex, and recent tomography studies (e.g. Rau and Wu 1995; Ma *et al.* 1996) have only just begun to provide some key details. Figure 3 shows two cross-sections through central Taiwan in our region of interest, using results of Rau and Wu (1995). The crustal root under the Central Range reaches a depth of about 50 km in the north and somewhat less toward the south. It is also clear that the rocks under the Central Range is in the range have velocities of 4.5–5.5 km sec^{-1}. The low-velocity sediments are confined mainly to the Coastal Plain. Under the Coastal Plain the crustal thickness is about 25–30 km.

The current orogeny of Taiwan is geologically quite young, with an estimated age of 4–6 Ma. The present Taiwan began to emerge above sea-level at that time (e.g. Liu *et al.* 2001). The rapid uplift rates of *c.*0.6–0.9 cm/year in the last 0.6 million years, based on fission-track dating (Liu *et al.* 1982) and >1 cm/year in the last 30 years based on repeated levelling data (Liu, C. C., Institute of Earth Sciences, Academia Sinica, pers. comm., 2002); these rates imply that vigorous orogenic processes are continuing.

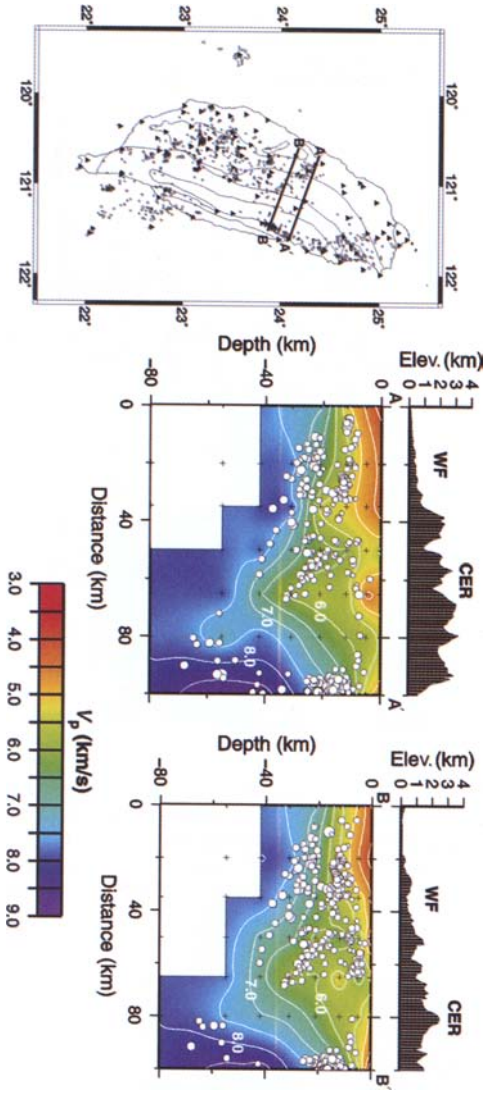

Fig. 3. Tomographic sections from Rau and Wu (1995). The locations of the profiles are shown in the figure, on the left. In both sections A–A′ and B–B′ the deepest part of the crust is nearly 50 km (as marked by the 7.5 km sec^{-1} contour). Materials with 5.5–6.0 km sec^{-1} rise under the Central Range (CER) to within a few kilometres of the surface. Under the Central Range the 5.5 km sec^{-1} materials reach to within a few kilometres of the surface, but in western Taiwan, under the Foothills and the Coastal Plain, the relatively low-velocity materials are thick. Section B–B′ crosses the area where the fault displacements of Chi-Chi are at their maximum.

While it is the general view that the Taiwan orogen was created as a result of the convergence, or collision, of the Philippine Sea and Eurasian plates, its exact geometry and the mechanics of mountain-building are debatable. Models proposed for the Taiwan orogeny include those of Suppe (1981), Lallemand *et al.* (2001), Carena *et al.* (2002) and Wu *et al.* (1997). The first three authors proposed models that involve eastward subduction of the Eurasian plate and deformation of the Tertiary sedimentary wedge to create the Central Range. However, Wu *et al.* argued that no subduction has been identified and that collision involves the shortening of the whole lithosphere. The seismicity data that we present here should provide further information for constraining these models.

Earthquake data in Taiwan

The two seismic networks mentioned earlier have supplied the seismic data pertinent to the current study. The 72 stations of the Central Weather Bureau (CWB) narrowband (centred around 1 Hz) network are located on Taiwan and its neighbouring islands (Fig. 2). All stations are equipped with three-component seismometers, and the signals are digitized on-site at the rate of 100 samples per second. The 12-bit data are then transmitted to the recording centre in Taipei. Although most of the stations are surface installations, at sites near cities a switch to borehole sensors at the depth of tens to over a hundred metres was made in July 1993; we only use data from after the switch. No significant differential time delays between stations were introduced in the transmission, and thus the relative arrival times, which double difference relocation relies on, are not affected by the transmission. The arrival times are read and used by the CWB for routine earthquake location and magnitude determination. Times are read with a precision of 1/100th of a second, determined by the sampling interval. The arrival times and the locations are archived at the CWB, and are used as the initial locations for our relocation program. For this study, all $M > 2$ events in the period July 1993 to the end of 2002, with a minimum of eight observations in a polygon (Fig. 1) are candidates for relocation. The other network of concern here is the BATS (Broadband Array in Taiwan for Seismology) network of the Institute of Earth Sciences (IES), Academia Sinica. Installation began in 1994, and by mid-1995 there were enough stations for waveform moment tensor inversion, from which the double-couple focal mechanisms can be derived. The station locations are shown in Figure 2. At each site, Streckeisen (STS-1 or STS-2) seismometers and digital data loggers are generally used. The BATS focal mechanism solutions are obtained for $M > 3.5$ events and published regularly (Kao *et al.* 2002). These results are used in this paper.

Double-difference relocation

Traditional earthquake location involves the adjustment of x, y, z and t_o, namely the three spatial coordinates and the origin time, to minimize the residuals between observed and calculated arrival times. The predicted arrival time is calculated on the basis of the Earth being a stack of layers with different velocities – a poor approximation to reality. The process is begun by assuming an initial trial location, and successive iterations are programmed to minimize the sum of the square of the residuals. In double-difference methods (Waldhauser 2001) the residuals in arrival times between events i and j (the double difference) are used. They are defined as:

$$\mathrm{d}r_k^{ij} = (t_k^i - t_k^j)^{\mathrm{obs}} - (t_k^i - t_k^j)^{\mathrm{cal}}$$

where 'obs' refers to observed, and 'cal' refers to calculated arrival times. For two events i and j we may write:

$$\frac{\partial t_k^i}{\partial m}\Delta m^i - \frac{\partial t_k^j}{\partial m}\Delta m^j = \mathrm{d}r_k^{ij}$$

where Δm^i is the adjustment of the hypocentral parameters (dx, dy, dz and dt) for event i; if the events are very close, then the same slowness can be used:

$$\frac{\partial t_k^{ij}}{\partial m}\Delta m^{ij} = \mathrm{d}r_k^{ij}$$

The resulting normal equation obtained from both the neighboring and the more distant events can be solved, if very large, by LQSR (Paige & Saunders 1982) and, for a small cluster of events, by using Singular Value Decomposition (SVD; e.g. Press *et al.* 1986).

To start off the iterated solution, the catalogue locations are used. In contrast to the routine earthquake location, in which each event location is determined independently, the double-difference relocation utilizes the fact that, if two events are very close, then the relative locations of the two events can be determined more efficaciously by the differences in arrival times at stations that record both events. By so doing,

the effect of the assumed velocity structures for calculating travel times is minimized. The formulation above also implies that the locations of the whole set of events are linked and that their relative locations with respect to an average location are determined by minimizing the squares of the double-difference residuals. The relative location should be quite good – within a few hundred metres (Waldhauser 2001).

A comparison of the CWB catalogue and the relocated seismicity

To demonstrate the effects of relocation, we present maps of epicentres, and five cross-sections each of both the CWB catalogue and the double-difference results for more than 6000 events in 2000 (Fig. 4). In the maps (Fig. 4a and 4c) the tightening of the epicentral clusters can clearly be seen after relocation. The five cross-sections in Figure 4b and 4d demonstrate how clouds of foci segregate into tighter groups. Compare, for example, the depth distributions (Fig. 4a and b, profiles 3) for a cluster of events just west of the Chelungpu fault at about 24°N, the relocated foci indicate a gently inclined east-dipping zone, while the catalogue results are quite scattered. Also, the relocated events under the Eastern Central Range in profile appear as a line of hypocentres, mapping a possible steep east-dipping fault. Although there is no a priori reason that tightly clustered foci are correct or better, the decrease in overall residuals and the improvement of formal location errors from a few kilometres to a few hundred metres, as well as the extensive demonstrations of Waldhauser *et al.* (1999) and Waldhauser & Ellsworth (2000, 2002), indicate that the tightly clustered results are meaningful.

Seismicity before and after the 1999 Chi-Chi earthquake

Pre-Chi-Chi seismicity

Seismicity. The Chi-Chi main rupture zone (e.g. Ji *et al.* 2001) had not been very active seismically before the Chi-Chi earthquake. In fact, only one moderately damaging event is known to have occurred there in the 1650–1999 period – the 1917 Puli event (Wu 1978). For the activity a few years before the Chi-Chi main-shock, we show the epicentral map and the cross-sections for the 1 July 1993–20 September 1999, seismicity in Figure 5a and Figure 6, respectively. One of the main features that can be recognized in Figure 5a was known since the first telemetered network was established in 1973 (Wang *et al.* 1983). This is the linear belt of seismicity that starts near the east-trending section at the northern end of the Chelungpu Fault, and continues south eastward for about seventy kilometres (Fig. 5a). It was often considered as a potentially hazardous seismogenic structure, and designated the Sanyi–Puli Belt (Lee *et al.* 1997; Wu & Rau 1998). A series of cross-sections parallel and perpendicular to this feature show that there are actually two zones: the upper one in the depth range of 5–15 km, and the lower one in the depth range 20 to 40 km; the top zone is flat or dipping to the south-west, and the deeper zone has a more complex structure and dips to the NE in places (Fig. 7). This zone essentially underlies the SW edge of the Hsuehshan Range and it is probably intimately related to the creation of the Range (see later discussion).

In the middle part of the region (Fig. 6, profiles 3–11) seismicity is relatively high in the Foothills, but noticeably low under the higher ranges; this gap under the Central Range has been recognized, although not as clearly, in earlier studies (Wu *et al.* 1989, 1997). As shown in Figure 5a the gap is essentially bounded by the western limit of the Backbone Range, or the Lishan fault as mentioned earlier. It is also defined clearly in profiles 4 through 12 in Figure 6. Seismicity does affect the region at higher elevation in profiles 1 through 3 and profiles 13 through 15. Interestingly, the events under the higher ranges are mostly above 10 km, explained elsewhere as a consequence of the rheological behaviour of rocks under the Central Range (Wu *et al.* 1997). In the southern part of the Central Range in our study area, we find a curious arch-shaped seismic zone under the Range, without much of a gap and with the events shallower under the high Central Range than on its flanks (Fig. 6, profiles 13, 14 and especially 15). In plan view (Fig. 5a) a series of relatively short (10–20 km in length) linear seismic zones can be seen under the high Ranges; they appear as narrow steep zones in cross-sections (Fig. 6, profiles 13–14). Along the coast of eastern Taiwan, between 24°N and 24.3°N the seismic zones are near vertical or dipping to the west, but in the Coastal Range – a region that has seen a few large earthquakes – the seismic zones are quite complex (Fig. 6, profiles 4–14). In some sections east-dipping zones dominate, but in others clearly west-dipping structures are displayed. In profiles 12 and 13 (Fig. 6), narrow east-dipping zones are quite clear.

Focal mechanisms. There are relatively few earthquakes, between July 1993 and the time of the Chi-Chi main-shock, in our study area that

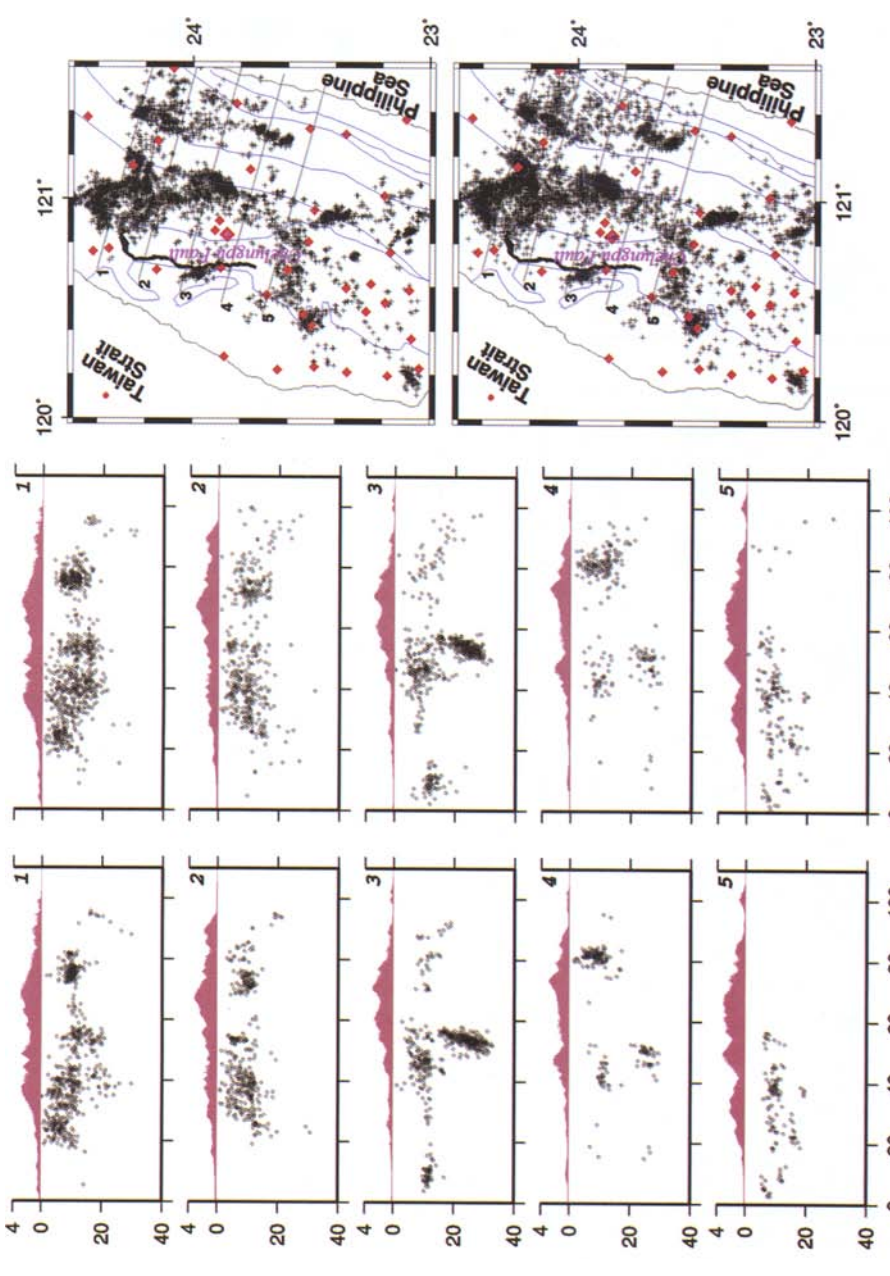

Fig. 4. Comparisons of the CWB catalogue and relocated event locations in plan view and in cross-sections. Aftershocks in 2000 are used. The five left-hand panels show the relocated events, and to their right the corresponding catalogue locations are shown; the locations of the profiles are shown in the maps on the right; the top figure shows the relocated and the bottom the catalogue epicentres. Note that the relocated events are more tightly clustered. In the two maps on the right, the top one shows the relocated and the bottom one the catalogue epicentres. The diamonds in this and later figures indicate the locations of the CWB network.

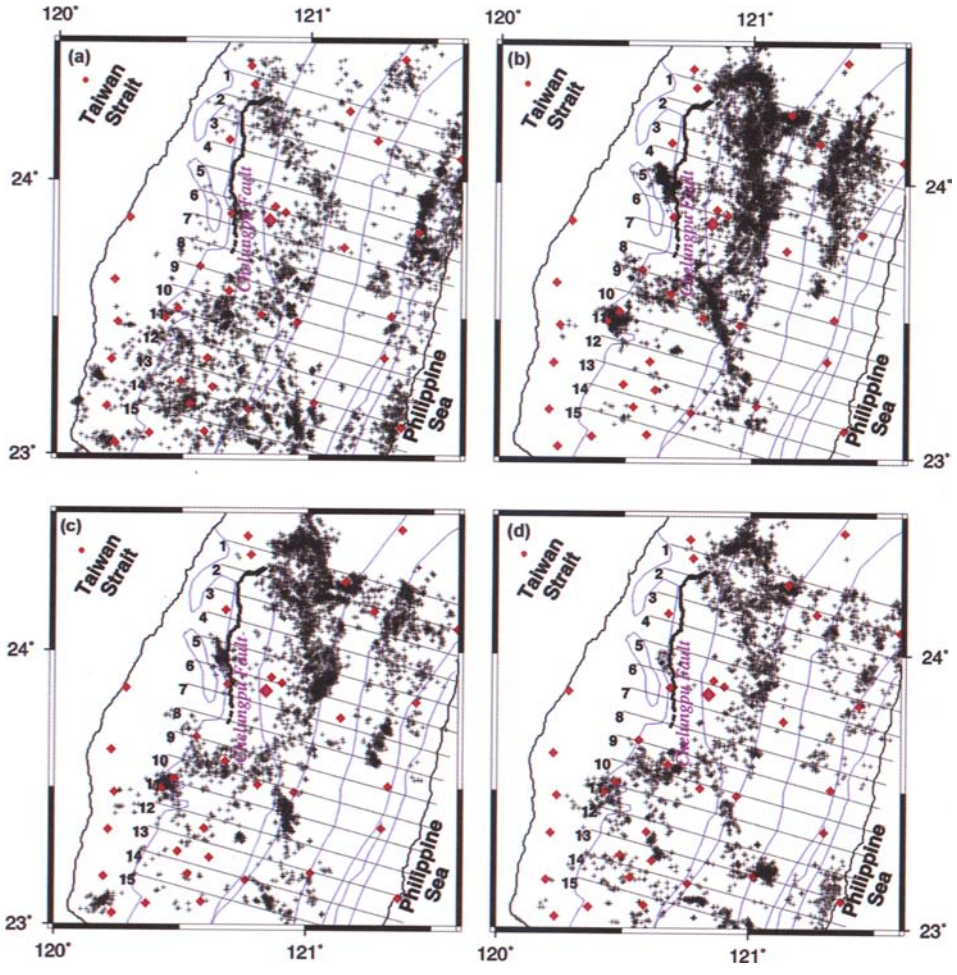

Fig. 5. Epicentral map of events in (**a**) 1 July 1993 to 20 September 1999, just before the Chi-Chi main-shock; (**b**) 20 September 1999, to 31 December 1999; (**c**) 1 January 2000, to 31 December 2000; (**d**) 1 January 2001, to 31 December 2002. Diagonal lines and numbers refer to cross-sections in Figures 6, 11, 12 & 13; for (**c**) there are no corresponding sections in other figures, but they are plotted on the map for reference.

are large enough ($M > 3.5$) for determination of focal mechanisms using BATS data (Kao *et al.* 2002). The mechanisms shown in Figure 8a are the BATS solutions, but they are placed at relocated epicentres; this is justified on the grounds that the moment tensor inversion results are not sensitive to a shift of a few kilometres in the location (H. Kao, pers. comm., 2003). We note that there was an $M3.7$ earthquake with nearly the same epicentre as the main-shock (Fig. 8a), but the BATS and the relocated depths of the event are both about 25 km, and thus much deeper than the Chi-Chi main-shock. It therefore cannot be considered a foreshock of the Chi-Chi earthquake. The largest earthquake in this period is the so-called 'Rueyli event' (mechanism 1998.07.04.51 in Fig. 9), about 30 km to the south of the southern end of the Chelungpu fault – the surface trace of the Chi-Chi earthquake fault. The fault plane solution and the hypocentral distribution favour the presence of an east-dipping plane. The solutions for events in the northern Longitudinal Valley are mainly high-angle thrust type, consistent with the focal distributions shown in Figure 6 (profiles 1–6 and 12–13).

Post-Chi-Chi seismicity

Since the main-shock, over 20 000 $M > 2.0$ aftershocks have been located by the CWB up to the end of 2002. The aftershocks immediately following

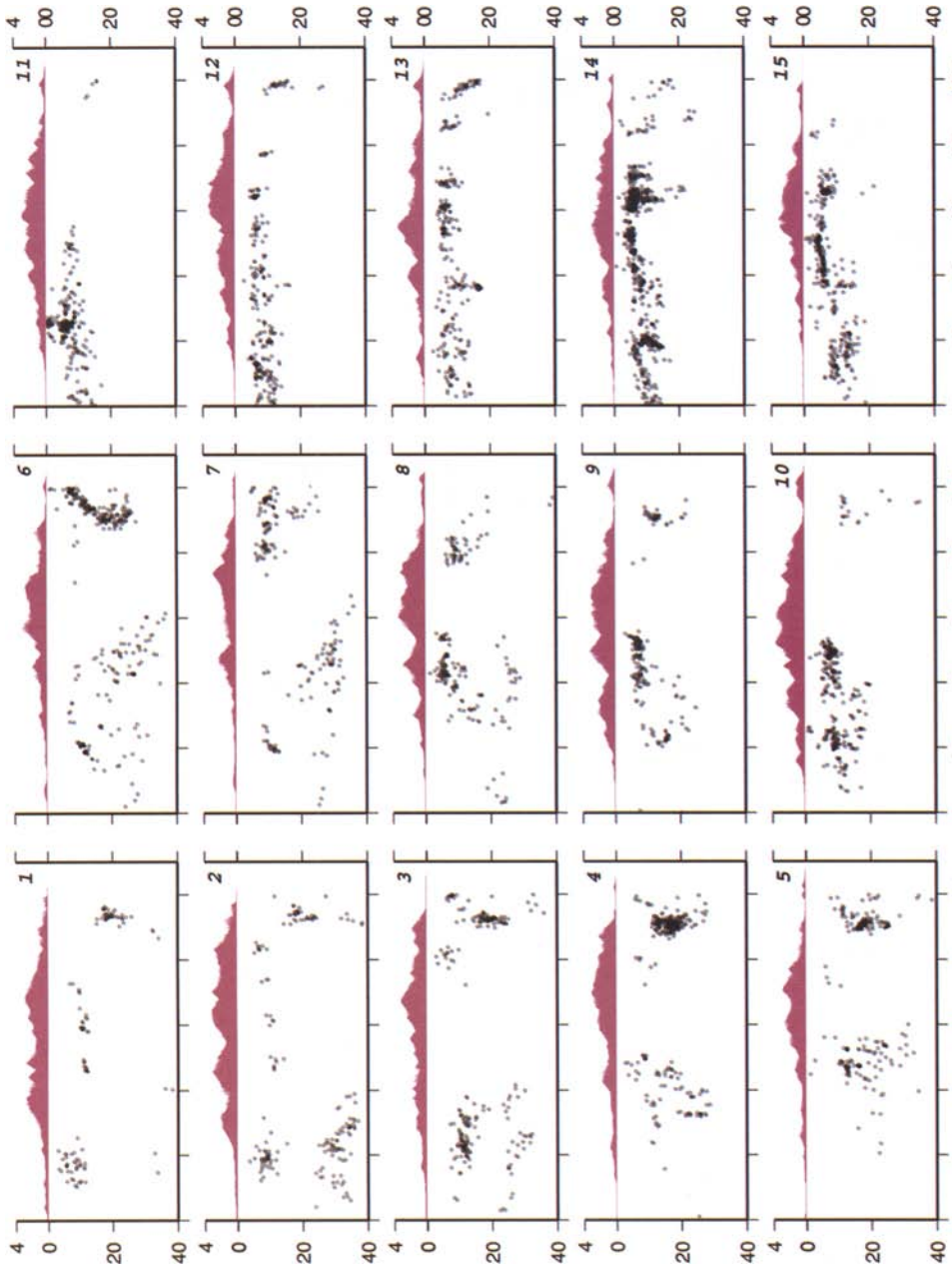

Fig. 6. Cross-sections of pre-Chi-Chi seismicity in Central Taiwan corresponding to Figure 5a. The locations of the profiles are also shown in Figure 5a. For each profile in this and later figures, events within 5 km on both sides of the profile are plotted. The profiles are 10 km apart. As in these and all the following sections, the horizontal axis is marked in kilometres from the end of the profile lines and the vertical axis is depth in kilometres.

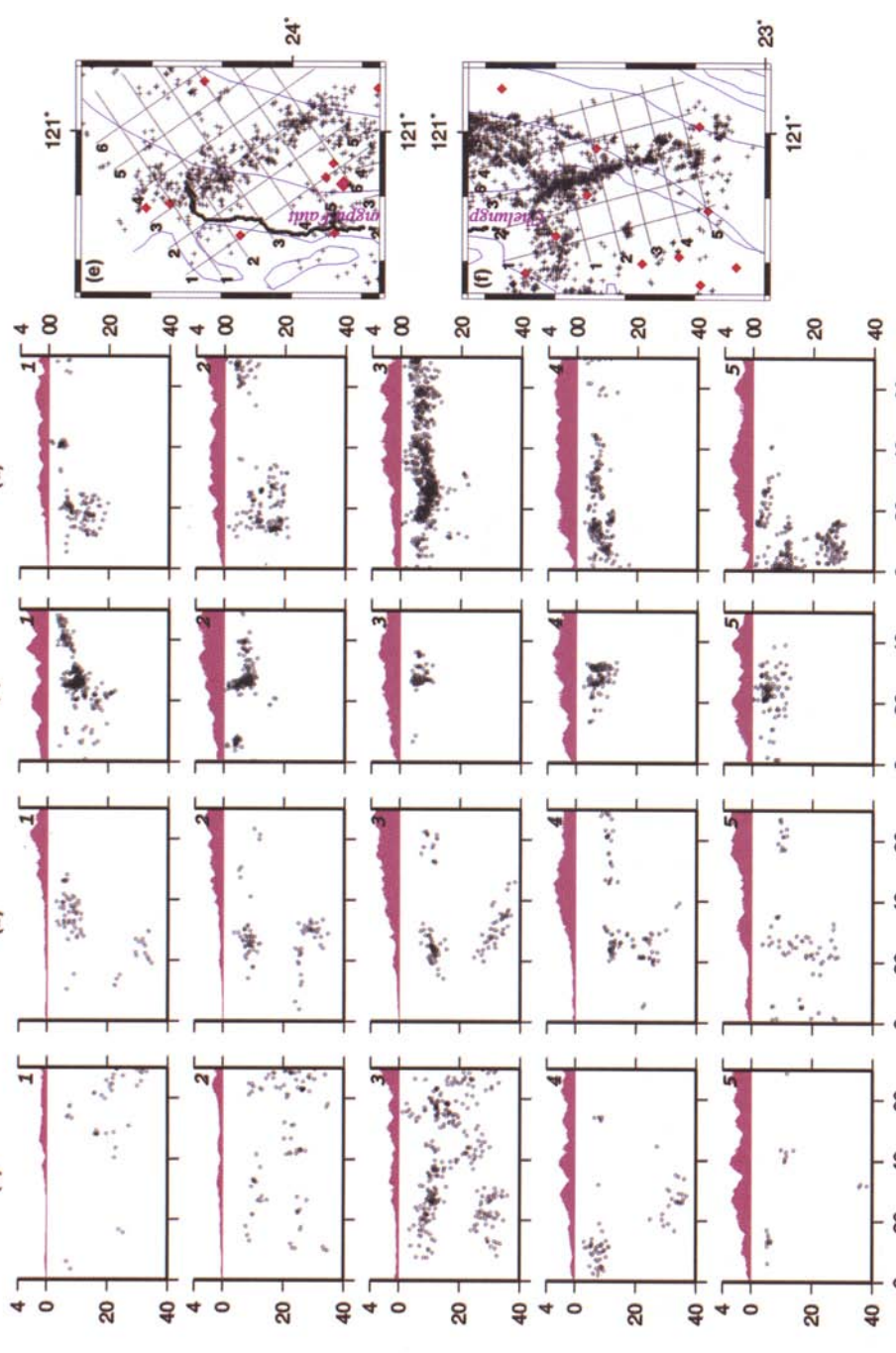

Fig. 7. Locations of profiles in two areas to show the details of two seismic zones. (**a**) Along strike of the Sanyi–Puli zone in northern Taiwan before the Chi-Chi main-shock; (**b**) Perpendicular to strike of the Sanyi-Puli zone before the Chi-Chi main-shock; (**c**) Along the strike of the Liliao Fault, 20 September 1999 to 31 December 1999; (**d**) Perpendicular to strike of the Liliao Fault, 20 September 1999 to 31 December 1999; (**e**) Epicentral map and location of profiles for the Sanyi-Puli zone; and (**f**) Epicentral map and location of profiles for the Luliao Fault.

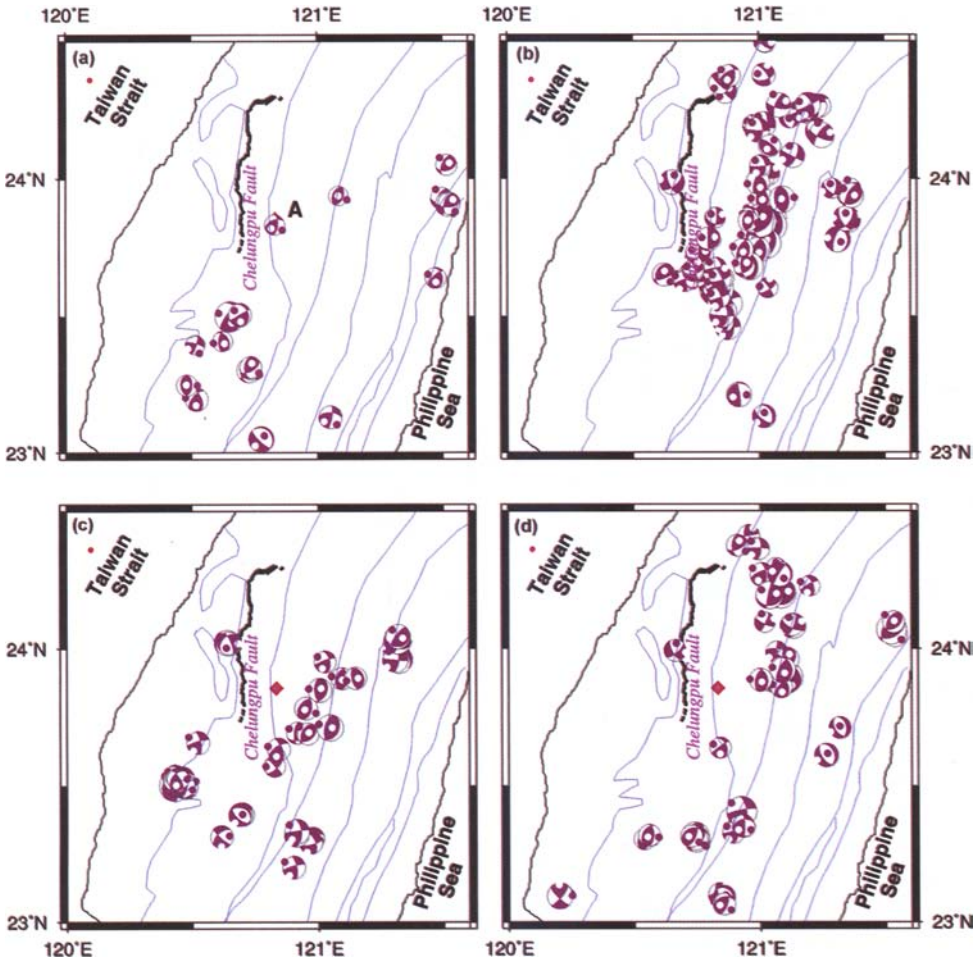

Fig. 8. Focal mechanisms of $M > 3.5$ earthquakes in the Chi-Chi area. (**a**) from 1996 to 1999, before the main-shock; event A occurred near the epicentre of the main-shock, but is at much greater depth; (**b**) from 20 September 1999, after the main-shock for 10 days; (**c**) 1 October to December 1999; (**d**) from 1 January 2000 to June 30, 2001.

the main-shock are so closely spaced in time that a portion of the events within the first ten days remains unlocated. But, with the majority of events already processed, future additions are not expected to alter the pattern of seismicity defined by the available events. From the time of the main-shock on 20 September 1999, to the end of 2000, 18 $M_w > 5.5$ events had occurred. Eight of them are listed in Table 1 with the USGS National Earthquake Information Center and our relocated hypocentres. Focal mechanisms for these events are available and, together with their own aftershock seismicity, seven of them can be associated with fault planes and particular types of faulting.

The post-Chi-Chi seismicity is shown in plan view in Figs 5b (20 September to December 1999), 5c (2000) and 5d (2001 and 2002). To see the initial development of the seismicity patterns, we have plotted the seismicity maps of September, October, November and December 1999, separately in maps (Fig. 10) with all post--Chi-Chi foci in 1999 shown together in cross-sections (Fig. 11).

Seismicity. In the first two and one half hours, the aftershock seismicity was limited to the east of the Chelungpu Fault, west of the Lishan Fault (Fig. 1), and above 13 km or so. Events in this zone continued to be the dominant seismicity in this area for the next two years. However, in the main rupture area, as indicated by the results of dynamic fault modelling (Ji *et al.* 2001;

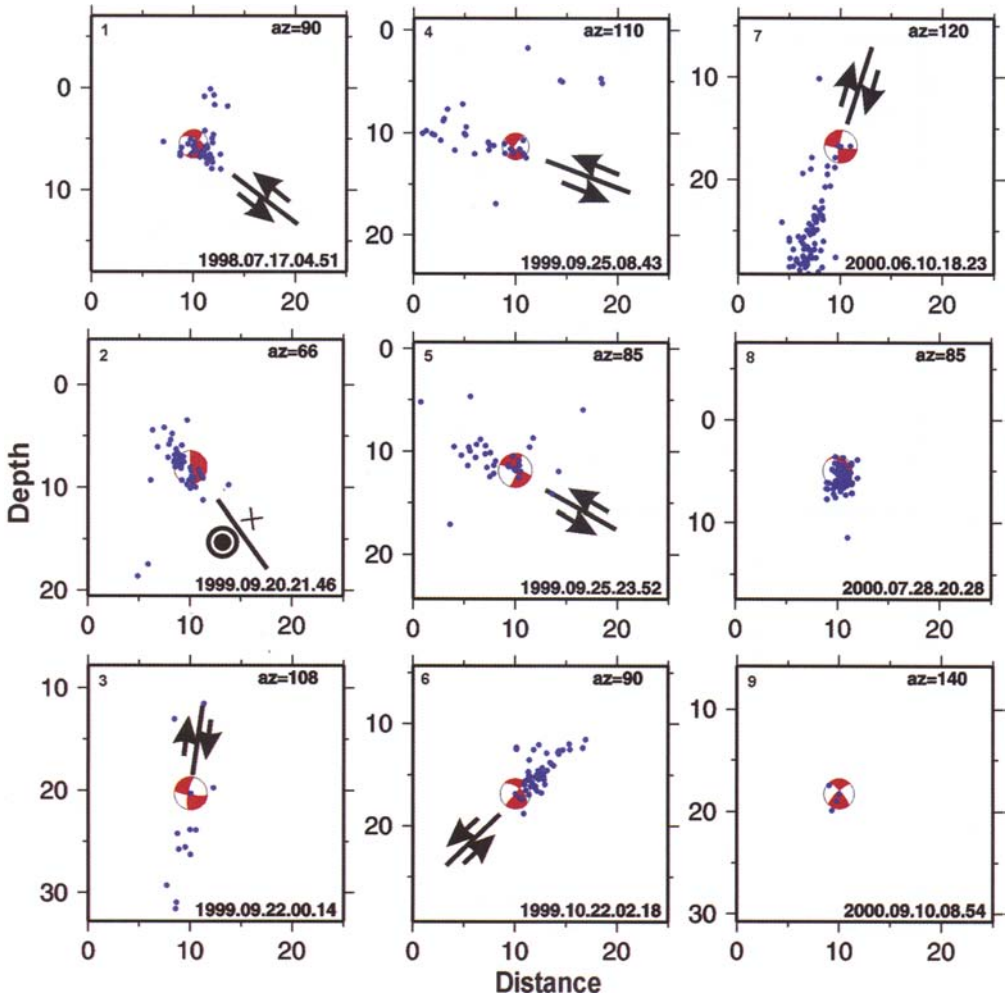

Fig. 9. Harvard CMT (all but 1999.09.25.08.43, which is a BATS solution) focal mechanisms for $M_w > 5.5$ events. The first 2–24 hours of aftershocks after each earthquake are plotted in the same frame. The date, hour and minute for each event are shown at the lower right-hand corner; the azimuth of the profile in the upper right-hand corner and the preferred fault orientation and movements are shown by a line and also by arrows. For events 8 and 9, too little information is available to decipher the associated fault.

Ma *et al.* 2001), directly east of the Chelungpu Fault, the aftershock activities were noticeably lower. The high activity concentrates mainly beyond the eastern edge of the rupture zone. We shall refer to this zone as the Chi-Chi zone in further discussion.

By viewing the time-lapse seismicity display in maps and in sections, we have followed the evolution of the seismicity in more detail than we can show in this paper. Three remarkable developments began approximately two and a half hours after the main-shock. One is the appearance of an Eastern Central Range seismicity belt, skipping the intervening higher mountain ranges; the first shock (of $M > 2$) of this NNE-trending zone was located toward the south, but, within two days, the zone grew toward the north, and, within one month, the Eastern Central Range zone attained nearly the same length as the Chelungpu Fault (Fig. 10b). The southern part of the eastern zone is relatively narrow and dipping steeply toward the east (Fig. 11, profile 8). The northern part of the zone is more complex. In fact, a few days after the main-shock shallow seismicity developed across the Backbone Range as well (Fig. 10b and Fig. 11, profiles 1, 2 and 3).

Table 1. *$M_w > 5.5$ events from USGS/NEIS**

Number	Year	Month	Day	Hour	Minute	Second	Lat	Long	Depth	M_w
1	1998	7	17	4	51	15	23.5	120.65	5.49	5.7
2	1999	9	20	21	46	37.3	23.59	120.83	7.89	6.5
3	1999	9	22	0	14	40.8	23.83	121.05	23.22	6.4
4	1999	9	25	8	43	29.2	23.68	120.97	11.32	5.6
5	1999	9	25	23	52	49.5	23.85	121.01	11.47	6.5
6	1999	10	22	2	18	56.9	23.5	120.43	16.85	5.9
7	2000	6	10	18	23	29.5	23.89	121.11	16.77	6.4
8	2000	7	28	20	28	7.7	23.4	120.93	4.93	5.7
9	2000	9	10	8	54	46.5	24.07	121.52	18.27	5.8

* The locations are the hypoDD results.

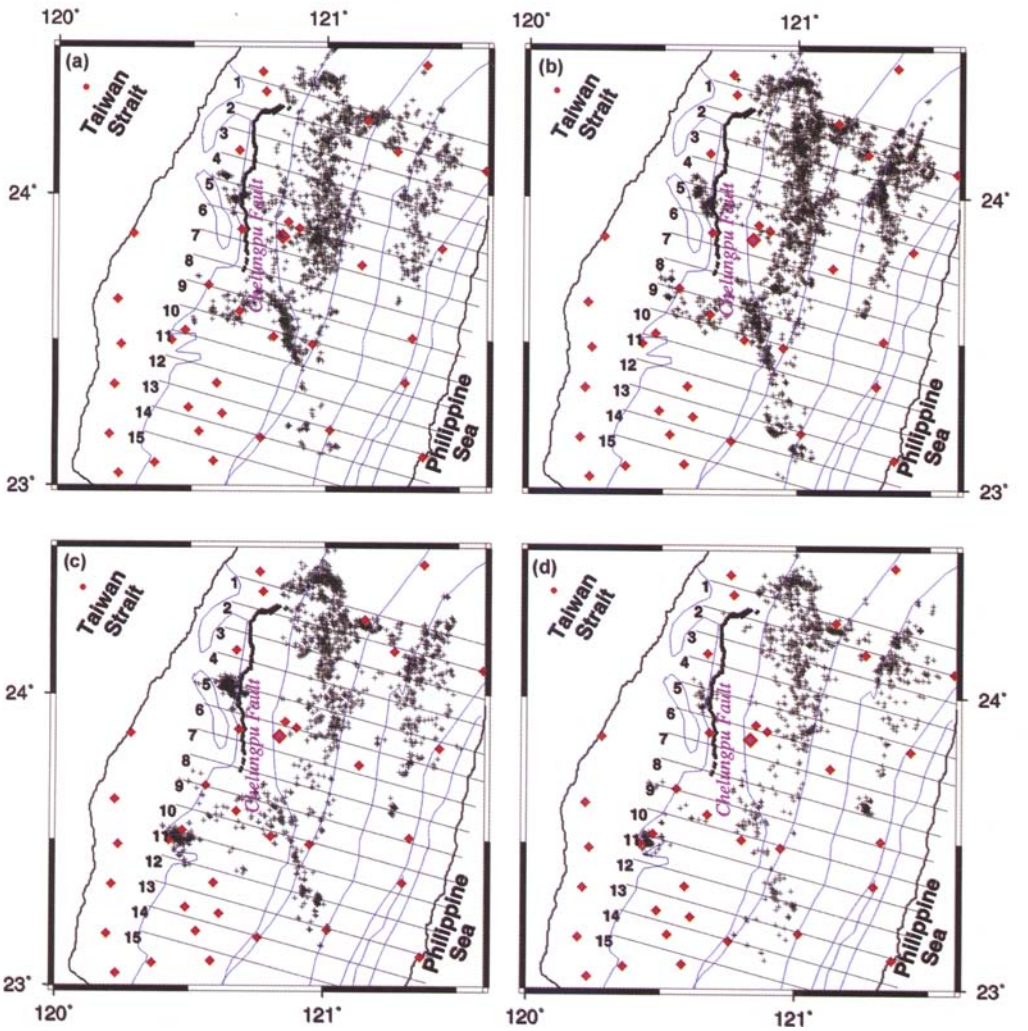

Fig. 10. Development of seismicity within the first hundred days of the Chi-Chi main-shock, as shown in epicentral maps in the following periods: (**a**) Within the first 11 days (from 20 September to 30 September 1999); (**b**) October 1999; (**c**) November 1999; (**d**) December 1999.

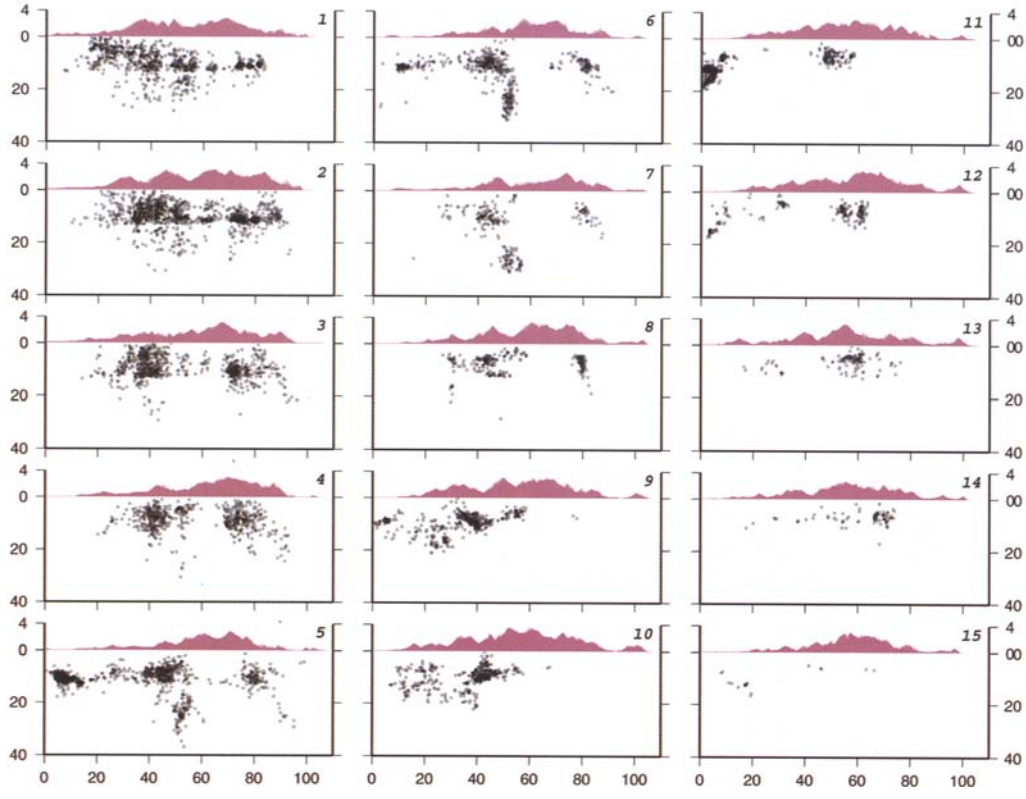

Fig. 11. Cross-sections of post-Chi-Chi seismicity from 20 September to 31 December 1999.

The pre-existing gap was bridged in this area, although the Backbone Range between latitudes of 23.3°N to 24°N was still quiescent, as shown in Fig. 5b. The seismicity in the eastern zone is evidently 'triggered' by the Chi-Chi main-shock, as earthquakes there began to appear within a few hours of the main-shock in an area that had been relatively quiet for many years.

The second remarkable development was the initiation of the lower crustal seismicity, between depths of 15 to 35 km immediately to the south-east of the main-shock zone (Fig. 4, profile 3; Figs 11 and 13, profiles 5 through 7). This zone, about 30 km long, dips steeply toward the west and strikes N–S; in the same profiles one can find other less-extensive zones to the west. Bounding the quiescent zone to the east and lying essentially under the Lishan Fault, this zone may play an important role in the orogen. Before the Chi-Chi earthquake, deeper earthquakes in this area did occur, but they were more scattered (Fig. 6, profiles 5, 6 and 7). At shallower depths (less than approximately 15 km) no corresponding zones of concentration under the Lishan Fault can be discerned; the western boundary of the quiescent zone is somewhat irregular (Figs 11 and 13, profiles 4–12).

The third development was the well-delineated, long and narrow belt of NNW-trending seismicity to the south of the Chi-Chi zone (Figs 5b, c and d). By taking sections along and across the zone, it can be seen that the zone dips steeply to the east and is contained mainly within the depth range of about 12 km (Fig. 7c, profile 2 and Fig. 7d, profile 3). This zone began to develop at its northern end, again within about two and a half hours of the main-shock, with its northern end connecting to the fairly complex zone of deeper crustal events (Fig. 7d, profile 5). It propagated southward for a distance of more than 50 km, and the seismicity is confined above *c.*13 km. This feature is somewhat unique, in that it cuts across geological boundaries, including the Lishan Fault. This zone has been linked to en echelon cracks on the ground (Li Yuanhsi, Central Geological Survey, Taiwan, pers. comm., 2003) and is identified as a part of the pre-existing Liliao fault.

The seismicity near the Chelungpu fault is very low, except for a group of events between

the Chelungpu and the Changhua Faults (Fig. 1 and Figs 5b, c and d). Activities began shortly after the main-shock, and continued through 2001. This cluster of aftershocks forms a shallow dipping zone (Fig. 11, profile 5 and Fig. 4, profile 3). When extrapolated to reach the surface, its trace would be about 20 km west of the Changhua Fault. However, the geometry of this zone may not be related to a thrust fault plane, as the focal mechanisms of the larger events show high-angle normal faulting (see below).

In the pre-Chi-Chi seismicity we have noted the presence of double-layered seismicity (e.g. Fig. 6, profiles 1, 2 and 3 in particular). But, in the corresponding post-Chi-Chi sections (Fig. 11, profiles 1, 2 and 3), the gaps are filled with events. After 2001 however, the gaps become visible again (Fig. 12, profiles 1, 2 and 3). However, it is interesting to note that even in the most active post-Chi-Chi period some of the basic features of seismicity remain. The seismically quiescent zone under the Backbone Range east of the Lishan Fault was clearly outlined during the first three months after the main-shock (Fig. 5b and Fig. 13, profiles 3–10). Later, in 2001–2002, more events were found there, but the shallow events dominated (Fig. 12, profiles 4 and 5). However, under the northern Longitudinal Valley and the Coastal Range, as well as in the Sanyi–Puli zone, seismicity was largely absent from the time of the main-shock until 2001.

Focal mechanisms and seismicity of $M > 5.5$ events. Of the $M > 5.5$ earthquakes after the Chi-Chi main-shock that are listed in the USGS/NEIS catalogue, many occurred within a few hours of the main event, or followed closely behind a previous large event, so that focal mechanism solutions for these events from either global or BATS data cannot be determined. For those with focal mechanisms, the choice of which of the two planes is the fault can be made with the relocated seismicity following the events. We have singled out nine events, including one in 1998, before the Chi-Chi earthquake, in the $M > 5.5$ catalogue obtained from the USGS/NEIS website for our study (Table 1). Except for one event (No. 4 in Table 1) Harvard moment tensor solutions are available; there are differences between some of the BATS and

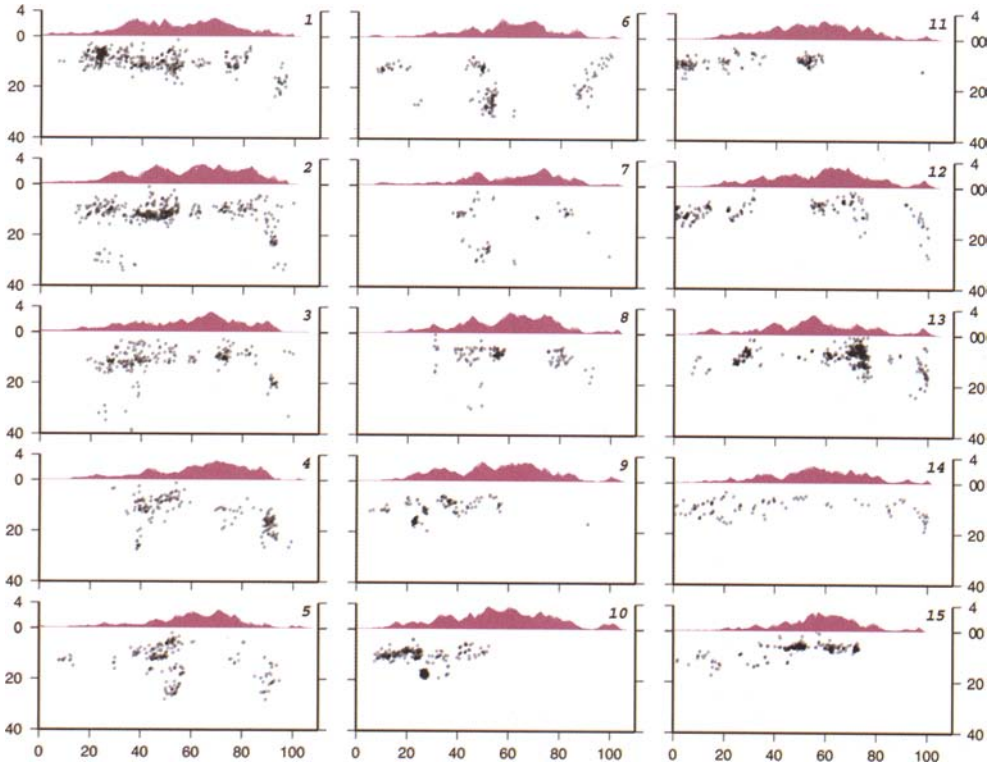

Fig. 12. Cross-sections of post-Chi-Chi seismicity for 2001 and 2002. For locations of the profiles, refer to Figure 5d. In profile 2 note the absence of earthquakes at depths of around 20 km.

Harvard solutions, but most of them are quite similar. We isolate the aftershocks within 48 hours after these events and show both the focal mechanisms and the relocated aftershocks in cross-sections (Fig. 9). The shocks are plotted at the locations determined in our study, in order to match the main-shock with the aftershocks; their location parameters and magnitudes are listed also in Table 1. We should note here that the teleseismic mechanism solutions are not sensitive to the relatively small adjustments in hypocentre locations in any case.

In Figure 9 event No. 2 is located near the northern end of the southern linear seismicity zone, or the Liliao Fault zone; the $M_w = 6.5$ event took place within four hours of the Chi-Chi main-shock. The seismicity lined up quite well in cross-section and on the map with the NNW-oriented left-lateral fault (Figs 7c, d and f; Fig. 8b); the Harvard CMT solution shows an essentially vertical plane, but the seismic zone is inclined (Fig. 9, no. 2). Events No. 3 and No. 7 are two of the deeper events, and the aftershocks indicate that the steeply west-dipping planes were the likely fault planes. Thus these two represent high-angle thrust fault, agreeing with conclusions made by Chen *et al.* (2002). The shallower events, No. 4 and No. 5, are associated with relatively shallow-dipping thrust faults, based on aftershock distributions. Event No. 6 was the main-shock that occurred to the west of the pre-Chi-Chi Rueyli earthquake (No. 1), quite distant and isolated from the main Chi-Chi seismic zone. It was preceded by a few foreshocks two days before the earthquake on 22 October. The aftershocks in the 24 hours after the main-shock clearly delineate a west-dipping zone, as shown in Figure 9 and also in Figure 11, profiles 11 and 12. The aftershock zone for event 8 is at the southern end of the Liliao seismic zone, and is evidently associated with a N–S-trending left-lateral strike-slip fault, but, as for event No. 9, too few aftershocks are present in the figures to define the fault plane dip.

Relation between BATS focal mechanism for $3.5 < M < 5.5$ events and seismicity. For smaller events, there is an abundance of BATS solutions in the few months after the main-shock. Figures 8b, c, and d show the results for September, October, and November plus December, respectively. The aggregate of thrust mechanisms in the area east of the Chelungpu Fault in Figure 8b shows that nearly horizontal E–W compressional stress (Kao and Angelier 2001) controls the tectonics in this region. The strike-slip faulting in the Liliao seismic zone is consistent with this stress field. However, there are several exceptions to this rule for events in the surrounding areas. Some of the clear exceptions are the normal faulting events with a E–W tensile stress axis in the Eastern Central Range, shown in Figures 8b and d. Furthermore, events west of the Chelungpu fault around 24°N also show similar mechanisms (Figs 8b, c, d). Although the events in these two regions have similar mechanisms they probably arise from totally different reasons, as we shall argue later.

Discussion: seismicity and brittle/ductile deformation of the Taiwan Orogen

While surface geology provides the boundary conditions for understanding a young mountain range, the earthquakes inside it can track a part of its internal deformation. The recognition of the deformation pattern is made easier when the catalogue locations of such events can be improved, as shown in Figure 4. Relocated hypocentres in Central Taiwan show a number of well-delineated zones. Some of these zones are nearly 'planar', conforming to our concept of fault zones. Certainly, each earthquake, large or small, has its own source zone and sense of motion. It is natural to assume that the distribution of the aftershocks in the first few tens of hours following a large event is related to the causative fault. Our results show that, in some cases, the alignment of earthquake foci within one or two days of the large event with one of the planes of the focal mechanism solution lends strong support to the choice of one of the planes of the mechanism solution as the fault plane. Experiences elsewhere (Waldhauser and Ellsworth 2000, 2002) show that the epicentres aligned very closely with the surface trace of faults. Figure 13 is the same as Figure 11, except that the interpreted faults based on seismicity and focal mechanisms are marked.

One of the clear features determined from the post-Chi-Chi seismicity is the deep crustal seismic zone. The epicentres of this zone lie very close to the Lishan Fault, and the steeply west-dipping zone lines up very closely with the steeply dipping plane of the focal mechanism solutions (both thrusts) of two large Chi-Chi aftershocks in this zone (Fig. 9, events 3 and 7) leaving little doubt that the rather intense seismicity in this zone is associated with a significant reverse fault at a depth of 20–35 km. Chen *et al.* (2002) also found this zone using their temporary network data, and call it a conjugate fault to the main Chi-Chi rupture. Since the compressive stress in this region is nearly horizontal (Kao and Angelier 2001), the angles between the main-shock rupture and the steep zone are quite

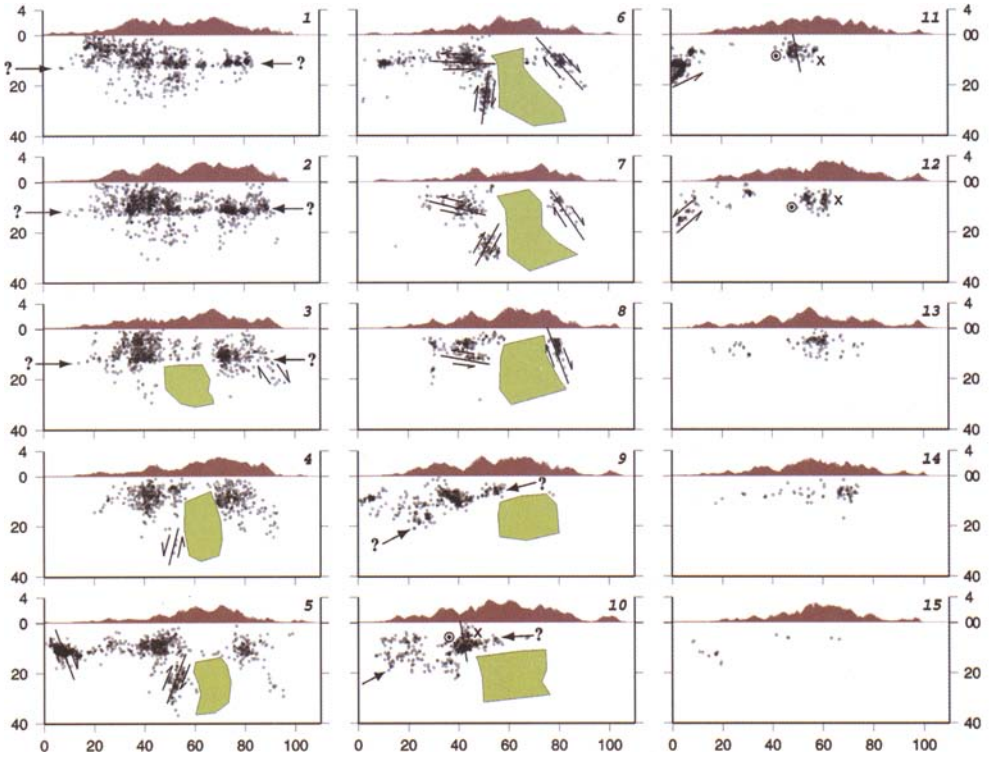

Fig. 13. Cross-sections of post-Chi-Chi seismicity from 20 September to 31 December; the data are the same as for Figure 11, except that an interpretation has been added. The arrow and question marks note the position of the discontinuity in the density of foci – much denser above the discontinuity than below it. Faulted areas are drawn with the sense of motion indicated. For a strike-slip fault: × indicates motion away from the reader and ⊙ motion toward the reader. The hatching indicates areas of seismic quiescence.

different, and they are not conjugate faults in the traditional sense. Conjugate or not, it is agreed that along this fault the Central Range is on the footwall side. It therefore does not help in the building of the Central Range. On the other hand, this fault does contribute to the creation of the root under the Central Range. It is known that Taiwan already has a substantial root (45–50 km thick) under the high ranges (Fig. 3), and motion along this fault could be a mechanism to bring the mid-crustal rock down to deeper level, as shown in Figure 13. Is the whole Range built in this way? So far, this presumed fault zone only extends for about 30 km in a north–south direction. However, these deep crustal earthquakes, occurring under the high temperatures that normally would inhibit seismicity, clearly show that significant deformation in that part of the crust in Taiwan is taking place. As far as the orogeny is concerned, the deepened root would lead to isostatic rebound, although, as has been argued elsewhere (Wu *et al.* 1997), pure shear deformation in the upper and the lower crust may ultimately be responsible for the morphogenesis; the multiple thrust faults in the upper crust under the eastern Foothills (Fig. 8b) may contribute to the rising of the Central Range.

The seismicity in the shallow part (< 10 km) of the Central Range presents a different situation. Before the main-shock, the seismicity in the southern part of our study area was apparently greater than further north, and it was nearly continuous across the southern Central Range. If thermal conditions control the seismicity further north, does a change in thermal conditions bring about the seismicity in this part of the Range? Two factors could be taken into consideration in this regard. First, this part of the Central Range is generally younger than further north-based on the geometry of the collision (Suppe 1981) or on the interpretation of palaeomagnetic data (Lee 1989). Therefore one may conclude that the deformation of this part of the Central Range may not have progressed as far as in the north, and therefore that the temperature is relatively

low at the top level. Secondly, the generally concave-upward shape of the zone of concentrated seismicity in this part of the Range, as shown in Figure 6, profiles 14 and 15, with the deeper foci under the Coastal Plain than under the high Central Range, is also consistent with the uplift of the Central Range and the elevated geotherm there, even though the top part is generally at a low enough temperature for the rocks to remain brittle. The variation in seismicity along the trend of the Central Range can thus be hypothesized as the result of a southward-propagating orogeny. A related question is: what does the Southern Central Range seismicity represent? Is the zone of concentrated seismicity related to the presence of a fault, following the interpretation of Carena *et al.* (2002)? But then the west-dipping plane would not fit Carena *et al.*'s prediction.

Among the differences between pre-Chi-Chi and post-Chi-Chi foci distributions is the mid-crustal (10–20 km) seismicity in some areas. The pre-Chi-Chi focal gap between the two zones of foci (Fig. 7, profiles 2, 3 and 4 in a and b) was filled with foci in the post-Chi-Chi period. There is a rather clear discontinuity at about 13 km (Fig. 11 and 13, profiles 1–3) in northern Taiwan; above this level the event density is evidently higher, but in the gap defined by pre-Chi-Chi seismicity there are a significant number of events after the main-shock. Then the two-layered seismicity became recognizable again in 2001 and 2002. Since the filling and emptying of the gap occurred over a period of more than a year, a cause related to the possible changes during this period must be sought. The most obvious process is that of a change in the stresses in the region as a function of time after the main-shock. Could the filling of this gap be an effect of the strain rate? In other words, just after the main-shock a sudden readjustment of stresses would have occurred, and during this period the rate of loading would be higher than the rate of tectonic loading in the pre-main-shock time; and thus the normally ductile materials became brittle (the 'silly putty' effect). Perhaps after 2001 the stresses had relaxed sufficiently and the materials in the gap became ductile. In contrast, the seismically quiescent Central Range did not seem to be affected by the assumed strain rate change; the zone remained essentially aseismic throughout the post-Chi-Chi period (Figs 11 and 13, profiles 4–10). With regard to the vertical discontinuity in seismicity itself, profiles 1–3 in Figure 11 show that it actually continues eastward to the Eastern Central Range, and is rather flat. It crosses regions with different geological characteristics at the surface, and most probably at depth, as indicated by the velocity changes across the Central Range in the tomographic velocity images (Fig. 3). The simplest explanation of this layering is that it is related to the level of groundwater circulation – controlled by gravity and porosity. It is conceivable that electrical conductivity from magnetotelluric studies may help to constrain such an interpretation, but at present it is difficult to be certain. The other possible explanation was that of Carena *et al.* (2002), i.e. it indicates the presence of a décollement, albeit one with a much limited spatial extent (only 30 km or so), in the N–S direction and one that is very flat all across the western Coastal Plain and the Eastern Central Range. This discontinuity in seismicity deserves further investigation.

Seismicity and its relation to brittle faulting in the orogen are obvious, but the easily recognized quiescent regions next to areas of high seismicity under parts of the Central Range east of the Lishan Fault require careful examination. Before the Chi-Chi main-shock, the presence of seismicity in the southern part of the Central Range in our study area is quite well defined (Figs 5a and 6, profiles 12–15); however, in the north (Figs 5a and 6, profiles 1 and 2) relatively few $M > 2$ earthquakes occurred under the Central Range, and they concentrated mainly above 10 km or so. In between these areas (Fig. 6, profiles 3–11) the Central Range is nearly aseismic, while the seismicity in the Foothills and the Coastal Range was comparatively high. This seismic quiescence is rather curious in view of the relatively high rate of uplift in the high Central Range. Wu *et al.* (1997) hypothesized that rocks under the high ranges are at a higher temperature, as a result of lower, hotter crustal materials having been elevated during the orogeny and thus leading to ductility of the rocks. Wu *et al.* also invoke the thermally induced ductility in quartzo-feldsparthic rocks (Kohlstedt *et al.* 1995) to explain the double-layered seismicity under parts of the Foothills; the double seismic layers can be seen in profiles 2, 3, 7 and 8 in Fig. 6. The presence of shallow seismicity in parts of the Central Range can be explained as a result of cooling of rocks, or perhaps due to the higher fluid pressure.

Tectonically, the double seismic zone whose details are shown in Figures 7a and 7b could be quite significant. Named the Sanyi–Puli Zone, it sits at the southwest edge of the Hsuehshan Range. For events in this zone, the focal mechanisms, as determined by Wu and Rau (1998), show both shallow and deep thrusts, striking generally in the NNE direction, but strike-slip and normal events are also present. So far, the events in this zone tend to be in the M2–3 range. If the deeper northwest-dipping zones seen in some profiles in Figure 7 do represent fault planes, and thrust

motion occurs on these faults then the Hsuehshan Range could ramp up on the lower thrust – similar to a mechanism proposed by Clark *et al.* (1993).

In terms of seismic zones activated after the Chi-Chi earthquake, the zone in the East Central Range is enigmatic. The zone is spatially distinct from the Chi-Chi zone, with the Central Range intervening, and most of mechanisms obtained for events in this zone are normal faults, with E–W tensile axes (Figs 8 & 13). Incidentally, these events are located in the same area where Crespi *et al.* (1996) found a number of normal faults in the outcrops of metamorphic rocks. Thus, this type of normal faulting had occurred during the lifetime of the Taiwan Orogeny – probably repeatedly. Normal faulting mechanisms for $M < 3.5$ events in recent times were not unusual (Rau *et al.* 1996), although there were not enough to define a major structure. Does large-scale normal faulting mainly occur after a large earthquake on the west side of the island? From the pattern of rapid after-slip following the mainshock (Hsü *et al.* 2002), the Backbone Range was moving faster westward than the Coastal Range (*c.*8 cm v. *c.*1–2 cm from September 1999 to December 1999), creating a post-earthquake stress field conducive to such faulting. The E–W tension also raises questions regarding how the compressive stresses in the Chi-Chi area are generated from the convergence of the Philippine Sea and Eurasian plates.

Yet another enigmatic zone is the cluster of events just west of the Chelungpu fault (Figs. 5b, 6b and 11, profile 5). In the profile, a shallowly west-dipping zone can be seen. However, the mechanisms as shown in Fig. 8b, c and d are all normal faulting mechanisms with E–W tensile axis and 45° planes. In the seismicity profiles there are steeply dipping features extending below the concentrated seismic zone. These are perhaps related to the 45°-dip normal faulting activities. The cur-

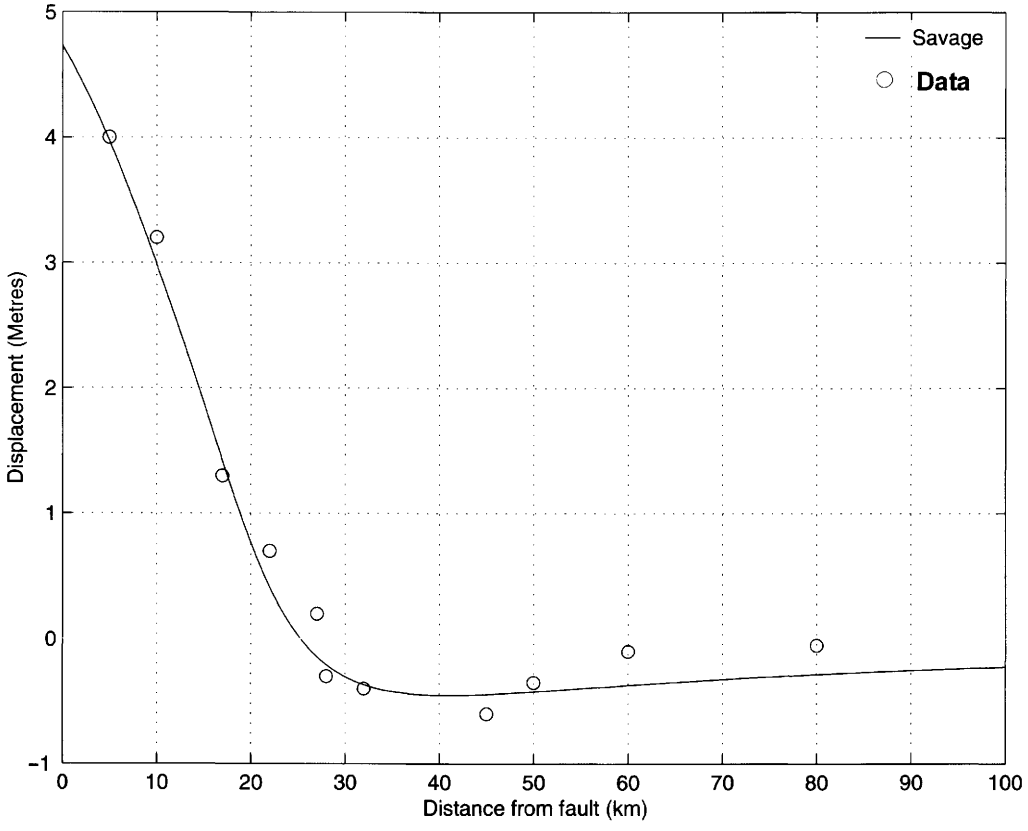

Fig. 14. Circles indicate vertical displacements of the hanging-wall side of the Chelungpu fault, along an E–W-profile at a latitude of 24.1°N with 0 on the fault. The data are sampled from Yang *et al.* (2000), and the line shows the theoretical displacement from a dislocation with a width of 20 km, dipping eastward at an angle of 25°, and the amplitude of displacement is 13 m.

ious juxtaposition of tensile and compressional faults calls for a mechanism that can switch the stresses within a fairly short distance. One consequence of the westward thrust along the Chelungpu fault by over 10 metres is that a wedge of mass was shifted in that direction. The addition of mass on the western crust may lead to flexure and therefore east–west tensile conditions in the upper crust.

Finally, judging from the deformation field accompanying the Chi-Chi faulting, one could say that the Chi-Chi earthquake itself did not contribute directly to the building of the Central Range. Yang *et al.* (2000) show that a part of the Backbone Range actually subsided about 1 m after the earthquake. A small part of this subsidence can be ascribed to the typical displacement field around a thrust fault; Figure 14 shows a fitting of the vertical displacement across an east–west section at 24.1°N across the Chelungpu Fault, showing the amount of subsidence expected from elastic rebound; the dislocation model (Savage 1983) used for the theoretical curve consists of a thrust fault 20 km wide, dipping at 25° and with a thrust displacement of 13 metres. While the theoretical model is a two-dimensional approximation of the fault, the parameters obtained are close to those obtained from dynamic modelling of the Chi-Chi fault (Ji *et al.* 2001; Ma *et al.* 2001). It illustrates the fact that the Chi-Chi earthquake itself led to subsidence beyond the buried tip of the Chelungpu Fault. The fault that the Central Range keeps on rising indicates the complexity of deformation in the orogen. The long-term uplift may very well be related to the ductile response of the crust.

Conclusion

The 1999 Chi-Chi earthquake in Taiwan activated a series of seismic zones, not only in the fringe area of the main rupture but also across the Central Range, to the south of the main rupture and to the lower crust east of the main rupture. Through the correlation of focal mechanisms of large and moderate earthquakes in these zones with their own detailed aftershock seismicity, the corresponding fault zones can be mapped. These faults and their senses of motion help us understand some of the deformation in the Taiwan orogen. A possible model for the creation of the root under the Central Range is thus proposed. The four-dimensional (space plus time) changes in the patterns of seismicity demonstrate the complex deformation in the orogen. Combining observations of presence and absence of seismicity and GPS (Yu and Chen 1994), it is clear that brittle deformation under the Foothills and ductile deformation under the Central Range are both important in the creation of the mountains of Taiwan (Hsu *et al.* 2003).

References

CARENA, S., SUPPE, J. & KAO, H. 2002. Active detachment of Taiwan illuminated by small earthquakes and its control of first order topography. *Geology*, **30**, 935–938.

CENTRAL GEOLOGICAL SURVEY OF ROC. 2000. *Geological Map of Taiwan*, 1:500,000, Central Geological Survey, Taipei, Taiwan.

CHEN, K. C., HUANG, B. S. & WANG, J. H. 2002. Conjugate thrust faulting associated with the 1999 Chi-Chi, Taiwan earthquake sequence, *Geophysical Research Letters*, **29**, (8), doi: 10.029/2001GL014250.

CLARK, M. B., FISHER, D. M., LU, C. Y. & CHEN, C. H. 1993. Kinematic analyses of the Hsuehshan Range, Taiwan; a large-scale pop-up structure. *Tectonics*, **12**, 205–218.

CRESPI, J. M., CHAN, Y. C. & SWAIM, M. S. 1996. Synorogenic extension and exhumation of the Taiwan hinterland. *Geology*, **24(3)**, 247–250.

DE METS, C., GORDON, R. G., ARGUS, D. F. & STEIN, S. 1990. Current plate motions. *Geophysical Journal International*, **101**, 425–478.

HO, C. S. 1988. *An Introduction to the Geology of Taiwan: Explanatory Text of the Geologic Map of Taiwan.* Central Geological Survey, the Ministry of Economic Affairs, Taipei, Taiwan.

HSU, Y. J., BECHOR, N., SEGALL, P., YU, S. B. & KUO, L. C. 2002. Rapid afterslip following the 1999 Chi-Chi Taiwan earthquake. *Geophysical Research Letters*, **29**, (16), 1754, doi: 10.1029/2002GL014967.

HSU, Y. J., SIMONS, M., YU, S. B., KUO, L. C. & CHEN, H. Y. 2003. A two-dimensional dislocation model for interseismic deformation of the Taiwan mountain belt. *Earth and Planetary Science Letters*, **211**, 287–294.

JI, C., HELMBERGER, D. V., SONG, T. R. A., MA, K. F. & WALD, D. J. 2001. Slip distribution and tectonic implication of the 1999 Chi-Chi, Taiwan, earthquake. *Geophysical Research Letters*, **28**, 4379–4382.

KAO, H. & ANGELIER, J. 2001. Stress tensor inversion for the Chi-Chi earthquake sequence and its implications on regional collision. *Bulletin, Seismological Society of America*, **91**, 1028–1040.

KAO, H. & CHEN, W. P. 2000. The Chi-Chi earthquake sequence; active, out-of-sequence thrust faulting in Taiwan. *Science*, **288**, 2346–2349.

KAO, H. & WU, F. T. 1996. The 16 September 1994 earthquake (mb = 6.5) in the Taiwan Strait and its tectonic implications. *Terrestrial Atmosphere Ocean*, **7**, 13–29.

KAO, H., LIU, Y. H., Liang W. T. & CHEN, W. P. 2002. Source parameters of regional earthquakes in Taiwan: 1999–2000 including the Chi-Chi earth-

quake sequence. *Terrestrial Atmosphere Ocean*, **13**, 279–298.

KOHLSTEDT, D. L., EVANS, B. & MACKWELL, S. J. 1995. Strength of the lithosphere: constraints imposed by laboratory experiments. *Journal of Geophysical Research*, **100**, 17 585–17 602.

LALLEMAND, S., FONT, Y., BIJWAARD, H. & KAO, H. 2001. New insights on 3-D plates interaction near Taiwan from tomography and tectonic implication, *Tectonophysics*, **335**, 229–253.

LEE, J. C., ANGELIER, J. & CHU, H. T. 1997. Polyphase history and kinematics of a complex major fault zone in the northern Taiwan mountain belt: the Lishan Fault. *Tectonophysics*, **274**, 97–115.

LEE, T. Q. 1989. *Evolution Tectonique et Geodynamique Neogene et Quaternaire de la Chaine Cotiere de Taiwan: Apport du Paleomagnetisme.* Thèse de Doctoral de l'Université Pierre et Marie Curie (Paris VI), Paris, France, 328 pp (in French).

LIU, T. K. 1982. Tectonic implication of fission track ages from the Central Range, Taiwan, *Proceedings Geological Society of China*, **25**, 22–37.

LIU, T. K., HSIEH, S., CHEN, Y. G. & CHEN, W. S. 2001. Thermo-kinematic evolution of the Taiwan oblique-collision mountain belt as revealed by zircon fission track dating. *Earth and Planetary Science Letters*, **186**, 45–56.

MA, K. F., MORI, J., LEE, S. J. & YU, S. B. 2001. Spatial and temporal distribution of slip for the 1999 Chi-Chi, Taiwan, earthquake, *Bulletin, Seismological Society of America*, **91**, 1069–1087.

MA, K. F., WANG, J. H. & ZHAO, D. 1996. Three-dimensional seismic velocity structure of the crust and uppermost mantle beneath Taiwan. *Journal of Physics of the Earth*, **44**, 85–105.

NORABUENA, E., LEFFLER-GRIFFIN *et al.* 1998. Space geodetic observations of Nazca-South America convergence along the Central Andes. *Science*, **279**, 358–362.

PAIGE, C. C. & Saunders, M. A. 1982. LSQR: sparse linear equations and least-squares problems. *ACM Transactions on Mathematical and Software*, **8/2**, 195–209.

PRESS, W. H., FLANNERY, B. P., TEUKOLSKI, S. A. & VETTERLING, W. T. 1986. *Numerical Recipes*, Cambridge Univ. Press, 818 pp.

RAU, R. J. & WU, F. T. 1995, Tomographic imaging of lithospheric structures under Taiwan. *Earth and Planetary Science Letters*, **133**, 517–532.

RAU, R. J., WU, F. T. & Shin,T. C. 1996. Regional network focal mechanism determination using 3D velocity model and SH/P amplitude ratio. *Bulletin Seismological Society of America*, **86**, 1270–1283.

RAU, R. J., LIANG, W. T., KAO, H. & HUANG, B. S. 2000. Shear wave anisotropy beneath the Taiwan orogen. *Earth and Planetary Science Letters*, **177**, 177–192.

SAVAGE, J. C. 1983. A dislocation model of strain accumulation and release at a subduction zone. *Journal of Geophysical Research*, **88**, 4984–4996.

SUPPE, J. 1981. Mechanics of mountain building and metamorphism in Taiwan. *Memoir of the Geological Society of China*, **4**, 67–89.

TENG, L. S. 1987. Tectostratigraphic facies and geologic evolution of the Coastal Range, eastern Taiwan. *Memoir of the Geological Society of China*, **8**, 229–250.

TSAI, Y. B., TENG, T., CHIU, J. M. & LIU, H. L. 1977. Tectonic implications of the seismicity in the Taiwan region. *Memoir of the Geological Society of China*, **2**, 13–41.

WALDHAUSER, F. 2001. HypoDD: a computer Program to compute double-difference hypocenter locations, US Geological Survey Open-File Report **01–113**, Menlo Park, California.

WALDHAUSER, F. & ELLSWORTH, W. L. 2000. A double-difference earthquake location algorithm: method and application to the northern Hayward fault. *Bulletin Seismological Society of America*, **90**, 1353–1368.

WALDHAUSER, F. & ELLSWORTH, W. L. 2002. Fault structure and mechanics of the Hayward Fault, California, from double difference earthquake locations. *Journal of Geophysical Research*, **107**, ESE 3-1–3-15.

WALDHAUSER, F., ELLSWORTH, W. L. & COLE, A. 1999. Slip-parallel seismic lineations on the Northern Hayward Fault, California. *Geophysical Research Letters*, **26**, 3525–3528.

WANG, J. H., TSAI, Y. B. & CHEN, K. C. 1983. Some aspects of seismicity in Taiwan region. *Bulletin Institute of Earth Sciences, Academia Sinica*, **3**, 87–104.

WU, F. T. 1978. Recent tectonics of Taiwan. *Journal of Physics of the Earth*, **26**, S265–S299.

WU, F. T. & RAU, R. J. 1998. Seismotectonics and identification of potential seismic source zones in Taiwan. *Terrestrial, Atmospheric and Oceanic Sciences*, **9**, 739–754.

WU, F. T., CHEN, K. C., WANG, J. H., MCCAFFERY, R. & SALZBERG, D. 1989. Focal mechanisms of recent large earthquakes and the nature of faulting in the longitudinal valley of eastern Taiwan. *Proceedings, Geological Society of China*, **32**, 157–177.

WU, F. T., RAU, R. J. & SALZBERG, D. 1997. Taiwan Orogeny; thin-skinned or lithospheric collision? An introduction to active collision in Taiwan. *Tectonophysics*, **274**, 191–220.

YANG, M., RAU, R. J., YU, J. Y. & YU, T. T. 2000. Geodetically observed surface displacements of the 1999 Chi-Chi, Taiwan, earthquake. *Earth Planets Space*, **52**, 403–413.

YEH, Y. T., LIU, C. C. & WANG, J. H. 2000. Seismic networks in Taiwan 1989. *Proceedings of the National Science Council, Republic of China, Part A: Physical Science and Engineering*, **13**, 23–31.

YU, S. B. & CHEN, H. Y. 1994. Global Positioning System measurements of crustal deformation in the Taiwan arc–continent collision zone. *Terrestrial, Atmospheric and Oceanic Sciences*, **5**, 477–498.

YU, S. B., KUO, L. C., PUNONGBAYAN, R. S. & RAMOS, E. G. 1999. GPS observation of crustal deformation in the Taiwan–Luzon region. *Geophysical Research Letters*, **26**, 923–926.